1 **Development and performance of a high-resolution surface wave and storm surge forecast model: Application**

2 **to a large lake**

3 **Laura L. Swatridge[1], Ryan P. Mulligan[1], Leon Boegman[1], and Shiliang Shan [1,2]**

4 [1] Department of Civil Engineering, Queen's University, Kingston, ON, Canada, K7L 3N6.

5 [2] Department of Physics and Space Science, Royal Military College of Canada, Kingston, ON, Canada,

6 K7K 7B4.

7 Correspondence to: Laura Swatridge (l.swatridge@queensu.ca)

9 **Key Points:**

10 • A real-time forecast model of wind-driven hydrodynamics in Lake Ontario is developed.

11 • Model performance compares well with observed data and other forecast models.

12 • Forecast lead time impacts the accuracy of wave height and storm surge predictions.

Abstract

A real-time forecast model of surface hydrodynamics in Lake Ontario (Coastlines-LO) was developed to automatically predict storm surge and surface waves. The system uses a dynamically coupled Delft3D – SWAN model with a structured grid to generate 48 h predictions for the lake that are updated every 6 h. The lake surface is forced with meteorological data from the High Resolution Deterministic Prediction System (HRDPS). The forecast model has been running since May 2021, capturing a wide variety of storm conditions. Good agreement between observations and modelled results is achieved, with root mean squared errors (RMSE) for water levels and waves under 0.02 m and 0.26 m, respectively. During storm events, the magnitude and timing of storm surges are accurately predicted at 9 monitoring stations (RMSE < 0.05 m), with model accuracy either improving or remaining consistent with decreasing forecast length. Forecast significant wave heights agree with observed data (1-12% relative error for peak wave heights) at 4 wave buoys in the lake. Coastlines-LO forecasts for storm surge prediction for two consecutive storm events were compared to those from the Great Lakes Coastal Forecasting System (GLCFS) to further evaluate model performance. Both systems achieved comparable results with average RMSEs of 0.02 m. Coastlines-LO is an open-source wrapper code driven by open-data and has a relatively low computational demand, compared to GLCFS, making this approach suitable for forecasting marine conditions in other coastal regions.

1 Introduction

Coastal regions of large lakes can face hazardous conditions with costly consequences due to strong storm events, where powerful winds generate large waves and storm surge (Danard, 2003; FEMA, 2014; Gallagher et al., 2020). Waves during these events can cause erosion, overtopping, and run-up, with the hazards being greater when the water level is elevated from storm surge. The intensity and frequency of strong storm events is increasing in the Great Lakes region as a result of climate change, as tropical storms are predicted to reach higher latitudes more often (Bender et al., 2010; Studholme et al., 2022). In addition, the mean water levels in the Great Lakes are being impacted by climate change, with large seasonal fluctuations in lake levels and record low and high water levels consistently occurring in recent years (Gronewold and Rood, 2019). The combined impacts of these projections present a greater risk for hazardous conditions in Great Lakes coastal regions, and developing better methods to understand and model the physical processes occurring during storms is important to help mitigate the risk. (Chisholm et al., 2021; Gronewold et al., 2013).

46

'Real-time forecasting' of lakes and coastal oceans can be achieved by applying numerical models to run predictive simulations of future hydrodynamic conditions in real time. Water level, circulation, and temperature simulations, using forecast models of large lakes and reservoirs, aid in water quality management (Baracchini et al., 2020; Carey et al., 2021; Lin et al., 2022). Coastal hazard forecasting is also being applied in numerous ocean regions, including the northern Gulf of Mexico where forecast systems of water levels and waves predict hurricane impacts on various scales (Bilskie et al., 2022; Dietrich et al., 2018; Paramygin et al., 2017). Similarly, Rey and Mulligan (2021) use a coupled Deflt3D–SWAN model to forecast storm conditions in coastal North Carolina, investigating the influence of various atmospheric forecast models on the results during hurricanes. Specific to lakes, the National Oceanic and Atmospheric Administration (NOAA) has implemented forecast models for North American coastal regions, including the Great Lakes, with the Great Lakes Coastal Forecast System (GLCFS). The GLCFS uses a high-resolution (30 m – 2 km) hydrodynamic model (FVCOM) to simulate physical processes including currents, temperatures, and water levels (Kelley et al., 2018; Peng et al., 2019). Waves in the Great Lakes are predicted by Environment and Climate Change Canada's (ECCC) Regional Ensemble Wave Prediction System (REWPS), which uses a probabilistic approach to forecast wave characteristic 3 days into the future.

Developing deterministic forecast models that run in real-time requires dealing with the challenge of minimizing the computational runtime of the model while still achieving accurate results (model resolution and performance), as the forecasts must be available in advance of the actual event. This need to effectively balance efficiency and accuracy in real-time models is an active research area (Elko et al., 2019). In addition, clear and efficient dissemination of forecasts must be provided to users and stakeholders. Typical real-time coastal models require large computing resources to run high resolution and accurate forecast simulations (Bilskie et al., 2022; Kelley et al., 2018), while fewer model applications focus on developing flexible systems that can achieve accurate results while running on local computers, often for smaller domains, using open data and with a smaller computational allowance (Lin et al., 2022; Rey and Mulligan, 2021).

The accuracy of numerical models for simulating the hydrodynamic response of coastal regions to storm events has increased with advances in computing power, data availability, and the development of models that can better represent more physical processes and their interactions, however model performance is still limited by the quality of input and forcing data available for a simulation. Model ability also depends on the grid resolution, with higher resolution models being more capable of resolving bathymetric features (Bilskie et al., 2022), and the inclusion of relevant processes, such as wave-current interactions and

80   baroclinic effects (Asher et al., 2019; Swatridge et al., 2022). A main consideration is the accuracy of the

81   atmospheric forcing, as winds are the primary driver of surface behaviour, and errors in the winds translate

82   through as errors in the modelled results (Dietrich et al., 2018; Farhadzadeh and Gangai, 2017; Rey and

83   Mulligan, 2021).

84

85   A probabilistic approach can be used to account for uncertainty in atmospheric forcing by running multiple

86   variations of the same event, however this requires large computational resources (Baracchini et al., 2020;

87   Fleming et al., 2008). In deterministic forecasts of water levels in Lake Erie, error in the atmospheric forcing

88   was significantly larger for 240 h forecasts compared to the 120 h forecasts, which translated to increased

89   error in predicted water levels (Lin et al., 2022). The longer forecast predicted excessive seiching and an

90   underestimation in peak water level, which improved as forecast length decreased. Forecasts of hurricane

91   storm surge and waves in the Gulf of Mexico by Forbes et al. (2010), Dietrich et al. (2018), and Bilskie et

92   al. (2022) found trends of decreasing error in storm surge prediction with shorter forecast length. Longer

93   forecasts (~5 days) resulted in storm surge variations of up to 4 m from the best track predictions, attributed

94   to variability in atmospheric forcing, and for forecasts shorter than 2.5 days, simulations converged on a

95   solution, and error was almost constant (Dietrich et al., 2018).

96

97   The hydrodynamics of Lake Ontario have been simulated on various scales in previous studies (e.g., Huang

98   et al., 2010; Paturi et al., 2012; Prakesh et al., 2007; Shore, 2009). Numerical models have also been used

99   to simulate waves and circulation during extreme events in the Kingston Basin (Cooper and Mulligan, 2016;

100 McCombs et al., 2014a; McCombs et al., 2014b). Sogut et al. (2019) used a combination of analyzing

101 historical water level and wave data, as well as numerical modelling of extreme storm events to gain insight

102 on lake seiching, storm surges, and wave patterns. Historical data have also been studied to determine the

103 risk of flooding due to storm surge along the Lake Ontario shoreline with a statistical model (Steinschneider,

104 2021). Surface waves and storm surge were simulated over the entire lake by Swatridge et al. (2022) during

105 recent storm events. Their study investigated the influence of different wind fields on the accuracy of storm

106 surge simulation, finding that variations in meteorological forcing were the primary source of uncertainty

107 in model results.

108

109 In the present study, an existing depth-averaged numerical model of Lake Ontario (Swatridge et al., 2022)

110 was applied to the lake to forecast water levels and waves in real-time, driven by spatially varied wind

111 fields from a high-resolution wind forecast model. The workflow develops an open-source Python- and

112 MATLAB-based wrapper code, that has been successfully applied to other systems using different

113 hydrodynamic models as part of the Canadian Coastal and Lake Forecasting Model System (Coastlines;

114   https://coastlines.engineering.queensu.ca; Lin et al., 2022; Rey and Mulligan, 2021). This flexible

115   methodology uses open access forcing/validation data and requires a relatively low computational demand,

116   compared to other existing Great Lakes storm surge models, allowing for application to other locations.

117   Model performance is evaluated by comparing results to near-real time observed data. Forecast results, for

118   storm surges and waves are statistically investigated over forecast lead times ranging from 6 to 48 h.

119

120   **2 Methods**

121

122   *2.1. Modelling Approach*

123   A two-dimensional (depth-averaged) coupled hydrodynamic-wave model is applied to Lake Ontario to

124   simulate wind driven hydrodynamics and waves using Delft3D-SWAN. The Delft3D flow model calculates

125   non-steady flow on a structured grid by solving the Reynolds-Averaged Navier Stokes equations (Lesser et

126   al., 2004). Wave conditions are simulated with the phase-averaged wave model, Simulating WAves

127   Nearshore (SWAN), which uses the spectral action balance equation to compute random wind-generated

128   waves. SWAN accounts for non-linear wave interactions, wave propagation, refraction, dissipation due to

129   whitecapping, bottom friction and depth-induced breaking (Booij et al., 1999). The models are dynamically

130   coupled to account for wave-current interactions. Radiation stress gradients from SWAN simulations are

131   input into the horizontal momentum equations in Delft3D to account for the impacts of waves on

132   circulation, such as wave-induced mass fluxes driving currents, and enhanced bed shear stress. Results from

133   the hydrodynamic simulation are then used to update water levels and circulation in the wave model.

134

135   Model setup choices were made based on simulations by Swatridge et al. (2022) which were adapted for

136   the present study to minimize computational demand, allowing the system to run in real-time. The Delft3D

137   simulation uses a curvilinear grid with a horizontal resolution gradually ranging from 250-450 m. The wave

138   grid has a coarser resolution, ranging from 350-600 m, thus reducing the computational time required to

139   complete a wave simulation while still achieving higher resolution in nearshore areas (Table S2 in the

140   supplementary material). Flow simulations are depth-averaged and barotropic, shown by Swatridge et al.

141   (2022) to accurately represent surface storm surge in Lake Ontario, with root mean squared errors (RMSEs)

142   between observations and model results ranging between 0.01 m - 0.07 m during several major events.

143   Bathymetry data was interpolated to the grid from the US National Centers for Environmental Information's

144   (NCEI) 3-arcsecond (~ 90 m) resolution dataset with supplementary data from the ETOPO1 global relief

145   model with a resolution of approximately 1.3 km (Fig. 1). Detailed sensitivity testing for this model was

146   completed in Swatridge et al. (2022) to calibrate model parameters. Hydrodynamic simulations use a time

147   step of 120 s to satisfy the Courant–Friedrichs–Lewy stability criterion, and coupling with the stationary

148   wave model occurs every 60 minutes.
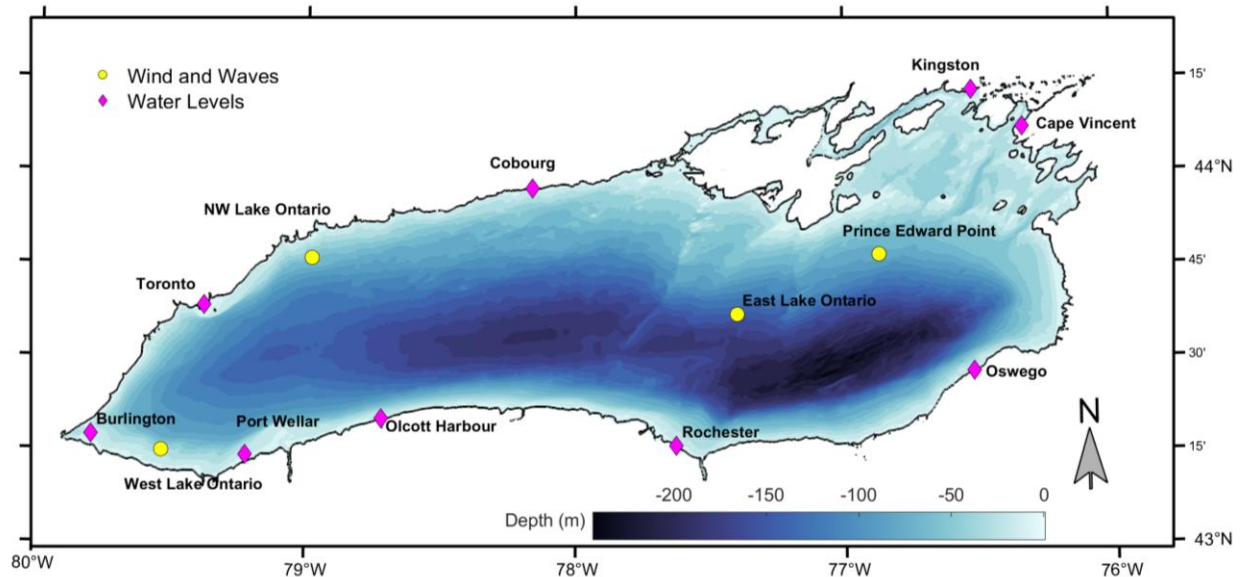
149

150   **Figure 1**: Map of Lake Ontario showing NCEI bathymetry and the location of real-time water level, wind,

151   and wave observation stations (Table 1, Table 2)

152

153   Spatially varied atmospheric input from the Meteorological Service of Canada (MSC) High Resolution

154   Deterministic Prediction System (HRDPS) is used to drive the model (Milbrandt et al., 2016). HRDPS is

155   an hourly assimilated forecast system downscaled from the larger scale Regional Deterministic Prediction

156   System (RDPS) that provides hourly predictions of surface pressure and wind velocity components with a

157   horizontal resolution of 2.5 km for the pan-Canada domain. The system runs every 6 h, predicting

158   atmospheric conditions 48 h into the future. This wind-forcing was successfully used by Swatridge et al.

159   (2022) to simulate the lake surface response to a range of storm conditions. Their modelled results for water

160   levels and surface waves agreed with observations at up to 16 locations in Lake Ontario, resulting in

161   maximum difference between predicted and observed peak wave heights and water levels of 0.4 m and

162   0.08 m, respectively. No lateral boundary conditions are applied to account for the influence of the riverine

163   flows (Niagara and St. Lawrence Rivers), as results from previous modelling studies have concluded that

164   the hydrodynamic influence of river inflows and outflows in limited to within 10 km of the river mouth,

165   and therefore can be neglected for simulations of lake wide water level over event based timescales.

166   (Prakash et al., 2007; McCombs et al. 2014a). The closed based approach leads to uncertainties in the

167   simulated results in the river region, however the impacts on the lake-wide hydraulics is expected to be

168   minimal.

169

170   *2.2. Development of an Automated Prediction System*

171   The forecast system uses a combination of code written in MATLAB and Python to automatically run every
172   6 h and has been operational since May 2021 (https://coastlines.engineering.queensu.ca/lake-ontario/). The
173   workflow (Fig 2) consists of pre-processing, model simulation and post processing stages. For pre-
174   processing, initiation of the modelling system is scheduled to occur when a new HRDPS forecast becomes
175   available. Python is used to download the latest forecast and MATLAB is used to automatically process the
176   atmospheric forcing and write input files for Delft3D-SWAN. The Delft3D model definition files are then
177   updated with the correct time information.
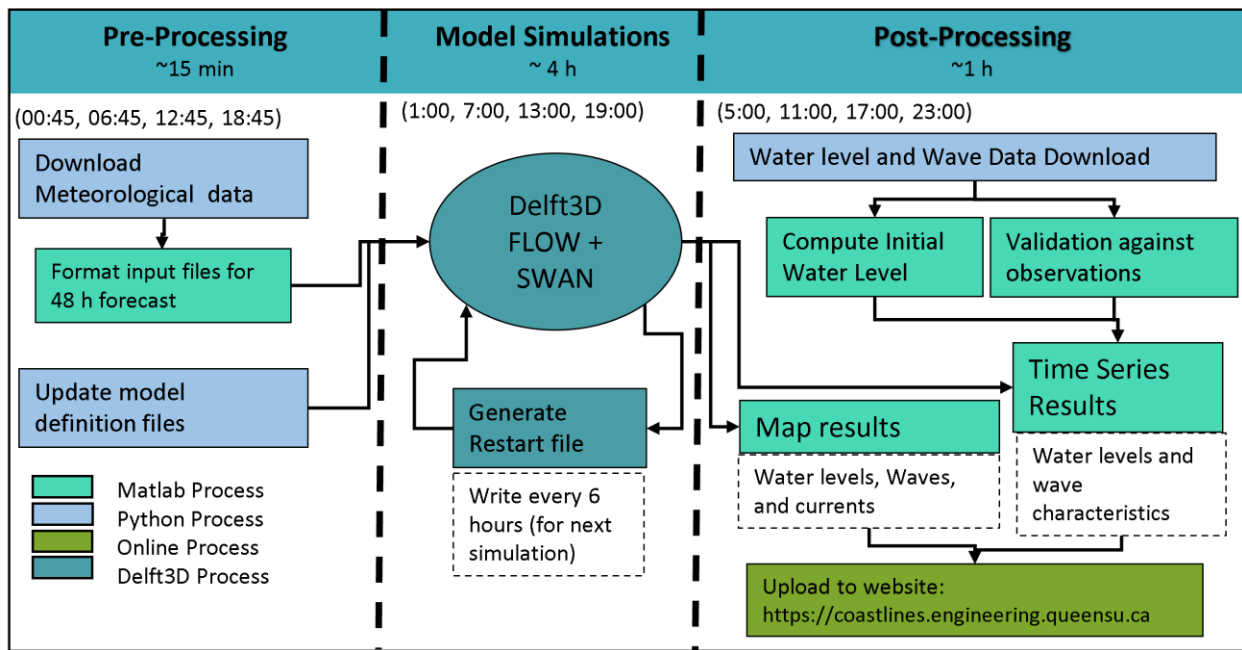
179   **Figure 2.** Diagram of the automated workflow for processes performed for each model cycle (every 6 h
180   initiated by Windows Task Scheduler) on the local Coastlines server.

182   Model simulations cover a period of 48 h and are 'hot-started' with a restart file from a previous model run
183   if available. If a restart file is not available, simulations begin from rest with initial water levels of 0 m and
184   current speeds (u) of 0 m s^{-1} throughout the lake. When the simulation finishes, all available real-time
185   observed data, outlined in Table S1 in the supplementary material, is downloaded using Python, which is
186   then processed in MATLAB. Observed water levels at each station are averaged over the previous 12 h and
187   used to locally adjust the datum of the model outputs. We acknowledge that assimilating observed water
188   levels into the initial conditions may be a preferred approach, but this is beyond the scope of the present
189   study and may be incorporated into future versions on Coastlines-LO. The model simulates high frequency
190   variability in water levels generated by winds. Seasonal changes in water levels due to inflows, outflows,
191   and evaporation are not included, but are accounted for in post-processing.

192

193 Time series plots of observed water levels and wave heights are automatically compared to the forecast

194 model results from the previous 2.5 days at the observation locations and additional plots are created to

195 provide predictions at other locations of interest with no observed data (Fig. 1). Spatial snapshots of model

196 results across the lake are generated at select times, as well as animations showing key output parameters

197 during the forecast simulation. All outputs are exported to Google Sheets and displayed on the project

198 webpage, https://coastlines.engineering.queensu.ca/. The system runs in a Windows environment using 16

199 cores of a 32-core XEON workstation, with each workflow cycle taking approximately 5 h to complete a

200 48 h forecast simulation.

201

202 *2.3. Real-time Comparison between Model Results and Observations*

203 Near real-time observations of water surface elevation (η) data are available at 9 water level gauges around

204 the perimeter of Lake Ontario from the National Oceanic and Atmospheric Administration (NOAA) and

205 the Department of Fisheries and Oceans Canada (DFO), with temporal resolutions of 3 minutes and 6

206 minutes, respectively (Fig. 1; Table 1). Hourly surface waves and winds are measured in Lake Ontario at

207 one US National Data Buoy Center (NDBC) buoy and ECCC buoys from spring to early winter (Table 2).

208 The buoys report the significant wave height (H_s), peak wave period (T_p), surface wind speed and direction

209 averaged over an 8-minute period (U).

210

211 **Table 1:** List of real-time water level gauge station locations

Name	Longitude	Latitude	Source
Oswego	-76.52	43.46	NOAA
Rochester	-77.63	43.27	NOAA
Olcott Harbour	-78.72	43.34	NOAA
Cape Vincent	-76.33	44.12	NOAA
Port Wellar	-79.22	43.24	DFO
Cobourg	-78.16	43.96	DFO
Burlington	-79.79	43.29	DFO
Kingston	-76.52	44.22	DFO
Toronto	-79.38	43.64	DFO

212

Table 2: List of real-time wave buoy locations

Name	Longitude	Latitude	Depth	Source
Prince Edward Point	-76.87	43.78	68 m	ECCC
West Lake Ontario	-79.53	43.25	35 m	ECCC
Northwest Lake Ontario	-78.98	43.77	54 m	ECCC
East Lake Ontario	-77.40	43.62	140 m	NDBC

For long term analysis of results, the residual component of the water level data, representing storm surge, is isolated at the gauge locations by finding the difference between the total water level and the average water level, calculated using a gaussian window of 7 days (Steinschneider et al., 2021). Model performance is quantified using statistical measures including the RMSE (eq. 1), normalized RMSE (NRMSE; eq. 2), and the correlation coefficient (r; eq. 3):

$$RMSE = \sqrt{\sum_{i=1}^{n} \frac{(x_i - y_i)^2}{n}} \tag{1}$$

$$NRMSE = \frac{RMSE}{\bar{y}} \tag{2}$$

$$r = \frac{\sum(y - \bar{y})(x - \bar{x})}{\sqrt{\sum(y - \bar{y})^2 \sum(x - \bar{x})^2}} \tag{3}$$

Where x_i and y_i (i = 1, 2, 3, … N) are time series of modelled and observed data respectively, and N is the number of samples in the series. ~~Strong s~~Storm surge events are identified from the water level data using the peaks-over-threshold method (Steinschneider et al. 2021). Forecast error during select events was evaluated by computing error metrics for consecutive forecasts leading up to the peak of the event. For each forecast, the relative error (RE; eq. 4), between observed and simulated maximum storm surge relative to the mean water level calculated at water level gauge locations, and between observed and modelled maximum wave heights at buoy locations was computed. The RMSE for each location was computed over a 6 h period that included the peak of the event.

$$RE = \frac{|(\bar{y} - y) - (\bar{x} - x)|}{(\bar{y} - y)} \tag{4}$$

3 Results

3.1. Long-term model performance

236   Simulation results, for water levels and waves, at the observation locations, were compiled over the 20-
237   month operational period. The first 6 h of each 48 h forecast were stitched into a single time series, and
238   these results were compared to the observed data (Fig. S1 in the supplementary material). During this time,
239   seasonal changes in the observed mean lake level fluctuated by over 1 m, with the highest water levels
240   occurring in May 2022. The ability of the model to reproduce storm surge was investigated over a four-
241   month period when multiple storm events occurred (106 days from 15 September 2022 to 30 December
242   2022; Fig. 3). Stations with larger ranges of observed water levels (i.e., Burlington, Cape Vincent), located
243   at the east and west ends of the lake (i.e., Fig. 3c, g) show a slight bias, where the model tended to slightly
244   overpredict the maximum and minimum values, corresponding to larger RMSE values (Table 3). These
245   stations also tended to show a stronger correlation (r = 0.83 − 0.86); whereas observation points with
246   typically smaller ranges in water levels (Fig. 3a, e) resulted in weaker correlations (r = 0.76 − 0.79).
247   Normalized results show comparable error statistics at all stations, with larger errors occurring at locations
248   with smaller storm surges (i.e., Rochester, Oswego).
249

250
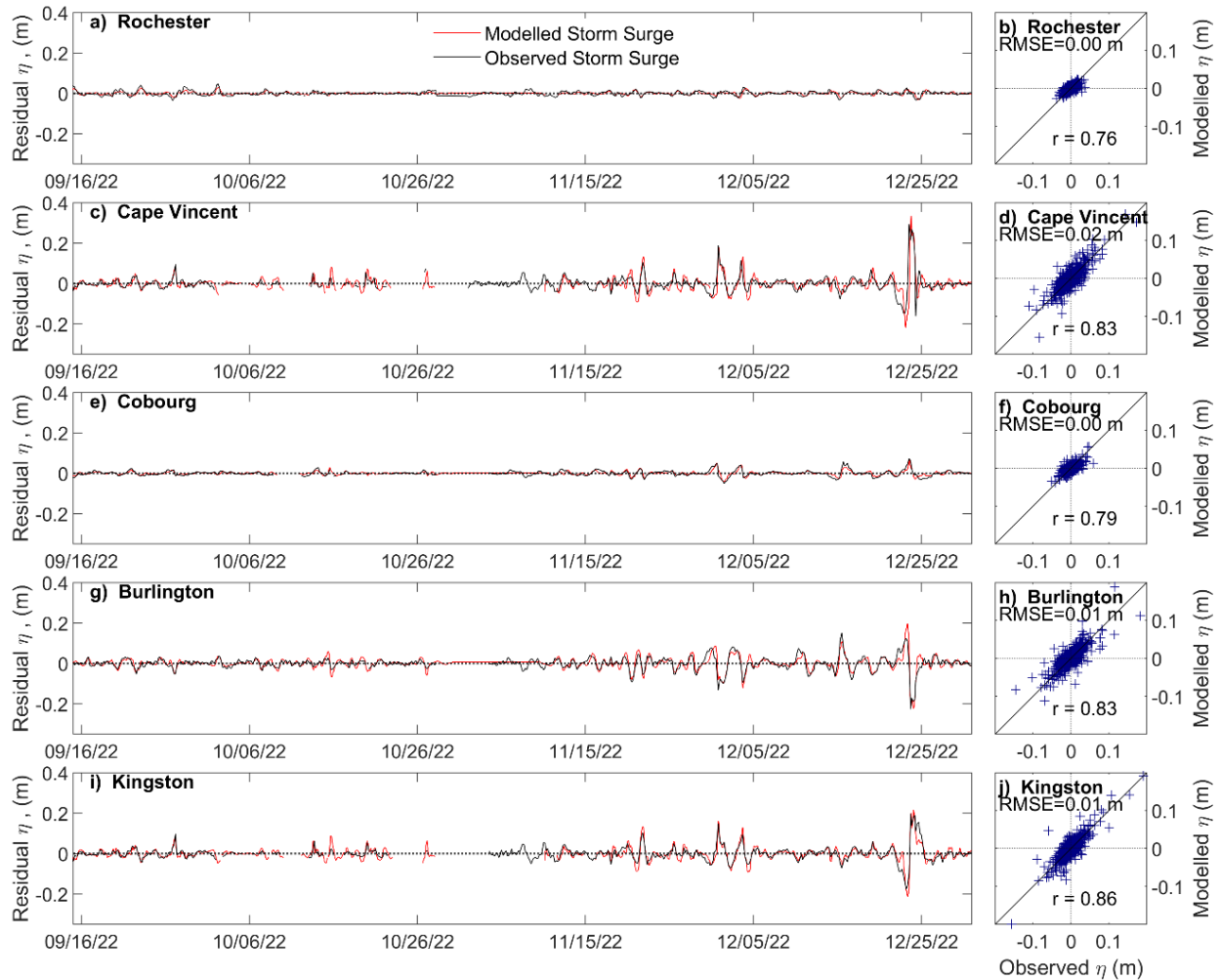
Figure 3: Observed (black) and modelled (red) residual water levels at select observation points over a 3 month period (September – December 2022) with corresponding scatter plots and error statistics over this period at select locations.

254

Table 3: Error Statistics for residual water level results over 106 days (September 15 – December 30, 2022)

	Minimum η (m)	Mean η (m)	Maximum η (m)	RMSE (m)	NRMSE (m)	r
Oswego	-0.10	0.07	0.12	0.01	0.15	0.80
Rochester	-0.03	0.03	0.04	0.00	0.16	0.76
Olcott	-0.16	0.04	0.11	0.01	0.19	0.80
Cape Vincent	-0.22	0.10	0.34	0.02	0.16	0.83
Port Wellar	-0.19	0.06	0.16	0.01	0.14	0.86
Cobourg	-0.08	0.04	0.07	0.01	0.14	0.79
Toronto	-0.16	0.07	0.14	0.01	0.14	0.83
Burlington	-0.22	0.10	0.20	0.02	0.14	0.83
Kingston	-0.21	0.09	0.25	0.01	0.14	0.86

Results for simulated H_s at buoy locations show the largest waves occurred during winter, between December and March (Fig.4). Results showing forecasted wave period compared to observations are shown in Fig S2 in the supplementary material. Over the 600-day operational period, no monitoring data was available for comparison and Lake Ontario could potentially experience partial ice-cover in nearshore areas, impacting the wave environment (Anderson et al., 2018). Stations in the eastern end of the lake (Prince Edward Point, East Lake Ontario) are expected to experience the largest waves due to the prominent north-easterly direction of storms over the lake, which results in winds blowing along the long-axis of the lake creating a large fetch at these locations (Lacke et al. 2007; McCombs et al. 2014a). Error statistics show similar values for RMSE at these points however Prince Edward Point had the lowest correlation coefficient (Fig. 4a, b; r = 0.71), while East Lake Ontario showed the highest correlation (Fig. 4c, d; r = 0.88). Lower RMSE were at stations with smaller waves (Fig. 4e, g), and normalized results (Table 3) show comparable results at all buoys (NRMSE = 0.42 – 0.53 m).

270
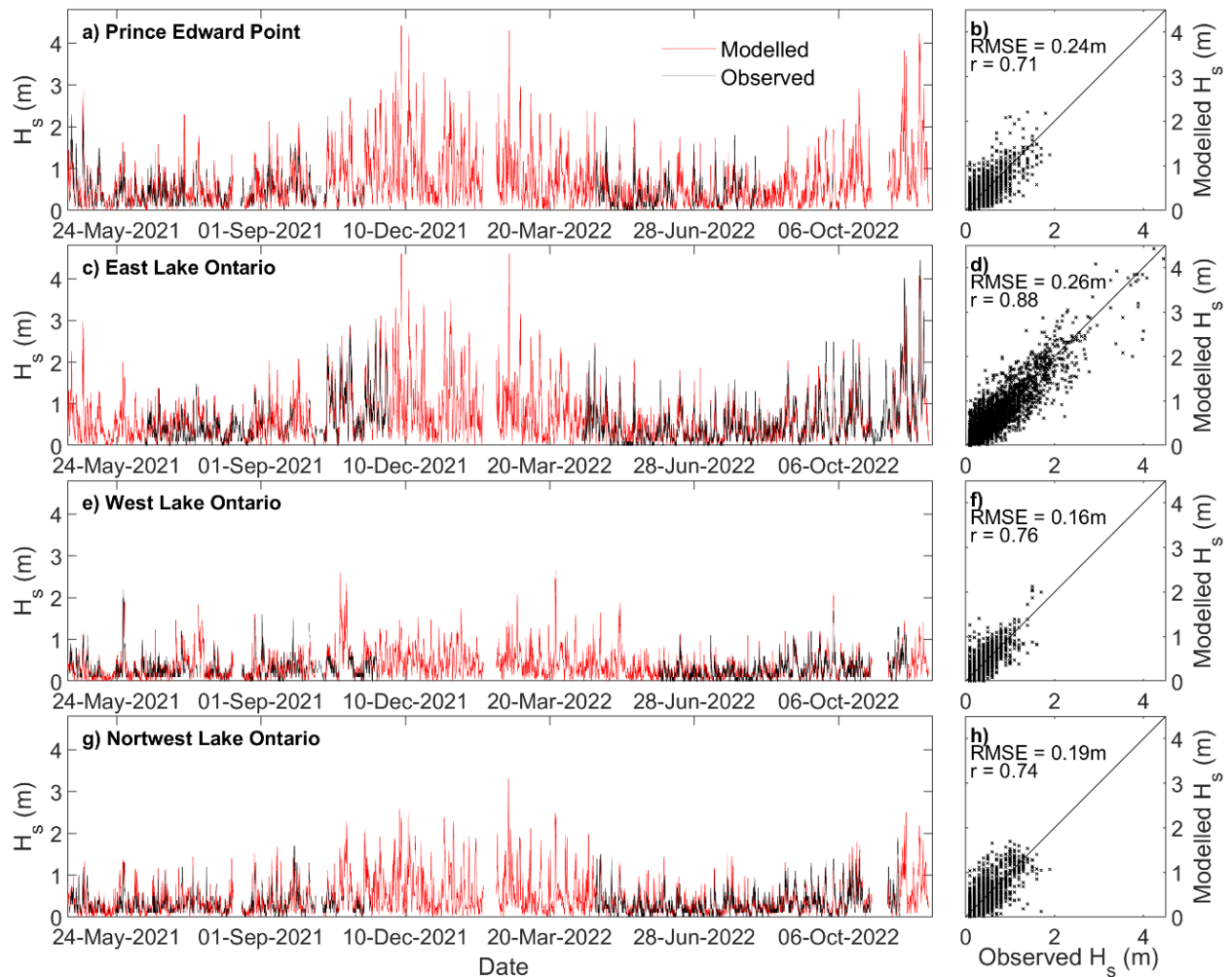
Figure 4: Time series of observed (black) and modelled (red) significant wave height over the duration that the buoys were in the lake (September -December 2022) with corresponding error scatter plots at the location of the 4 buoys. Note that the model was offline and are unavailable between February 9 – 27, 2022 due to a change of service for the meteorological inputs.

275

276 **Table 3:** Error statistics for significant wave heights at the buoy locations over 600 days (April 21, 2021 –

277 December 12, 2022)

Location	Mean H_s (m)	Maximum H_s (m)	RMSE (m)	r	NRMSE (m)
Prince Edward Point	0.44	3.82	0.24	0.71	0.53
East Lake Ontario	0.62	4.42	0.26	0.88	0.42
West Lake Ontario	0.34	2.60	0.16	0.76	0.48
Northwest Lake Ontario	0.35	2.29	0.19	0.74	0.53

278

279 *3.2. Storm event forecasts*

280 The performance of the model was evaluated over an event on November 11- 12 2021, consisting of wind

281 speeds that approached 15 m s-1, with the direction rotating clockwise from blowing towards the northeast

282 to the winds dominantly blowing towards the east over a 24 h period. This event was selected due to the

283 large storm surge generated ($\eta = 0.17$ m), and it resulted in the largest significant wave height that occurred

284 over the 20 month operational period with wave measurements available at~~from~~ all buoy locations for

285 comparison. Overlapping 48 h HRDPS forecasts (i.e., generated every 6 h) were validated against buoy

286 observations, with good agreement found between modelled and predicted total wind speeds and directions,

287 with peak wind speeds underrepresented by at most, 4.21 m s^{-1} at Northwest Lake Ontario and overpredicted

288 by up to 2.61 m s^{-1} at Prince Edward Point (Fig. S3 in the supplementary material)

289

290 This event resulted in an observed storm surge of up to 0.16 m in the northeast region of the lake, at Cape

291 Vincent and Kingston. The forecast simulations captured the timing and magnitude of the event peak, with

292 predicted surge values ranging between 0.12 m – 0.17 m (Fig.5d, i). A set down of about 0.10 m was

293 recorded at the Burlington station, which was underpredicted by the model by up to 0.05 m for the initial

294 forecast results, and improves as the forecast lead time decreases, to a prediction of 0.08 m. ~~~~The simulated

295 results at this location predicted water levels up to 0.05 m higher than the observations for the 24 h preceding

296 the storm (Fig.5h). Notable error can also be identified at Cobourg (Fig. 5f) with the model predicting

297 negligible fluctuations in the water surface, but observations show some oscillations (0.05 m).

298

299
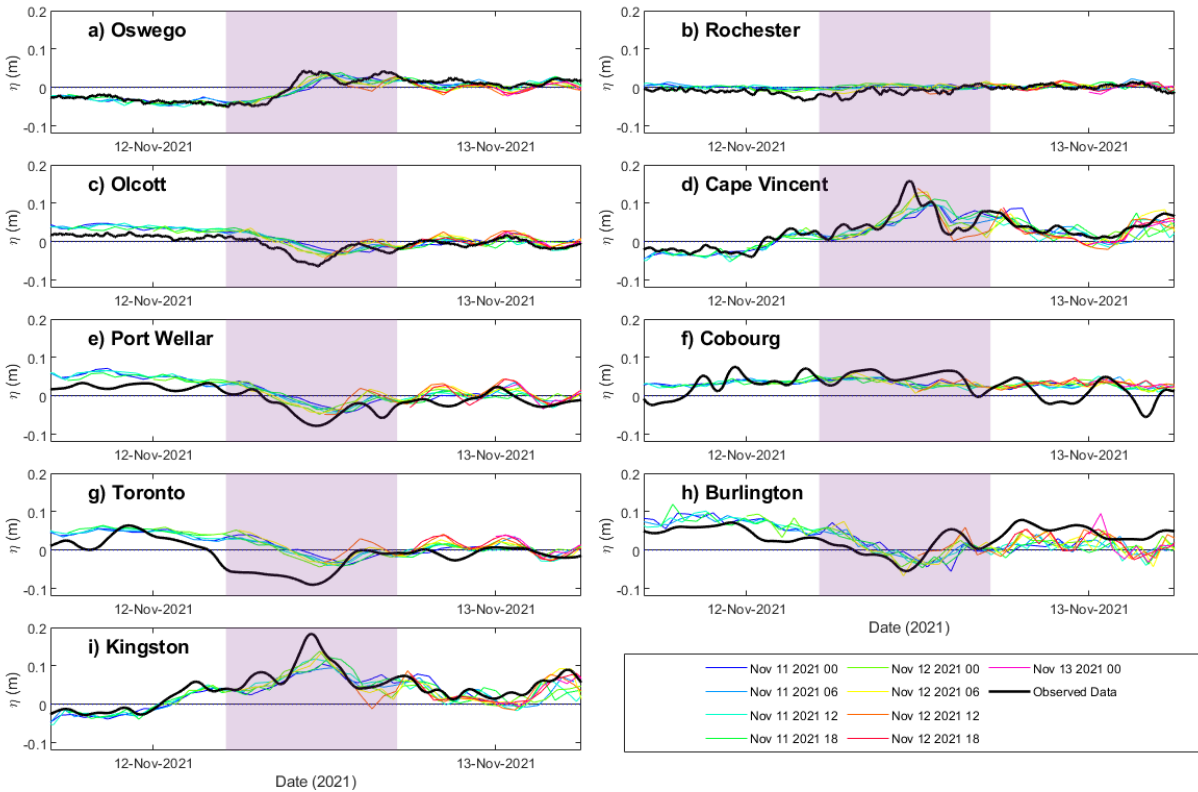
Figure 5: Time series of measured water levels at various observation points compared to forecasted data from progressive model simulations. The highlighted area indicates the 12 h period over which error statistics are computed.

303

Forecast performance was quantified by computing error statistics, over the duration of the event, for each forecast leading up to the time of peak water level. The largest errors occurred at the location of the set down, Burlington and Toronto, with a nearly constant RMSE of 0.03 m, and RE of 14% and 10% respectively (Fig. 6c, d). The errors at all stations remained fairly constant with RMSE and RE under 0.03 m and 10%, respectively, for each new forecast. However, map results showing the spatial variability in water level predictions from forecasts 12 h and 36 h before the storm peak show large differences (Fig. 6a,b). The earlier results (Fig. 6a) simulated a far less extensive storm surge in the northeast region of the lake than what was subsequently predicted 24 h later (Fig. 6b), when the storm surge was simulated to impact most of the northeast shoreline. The later forecast also predicted spatially larger set-down, about 0.10 m more than the earlier forecast in the western region of the lake.

314

315
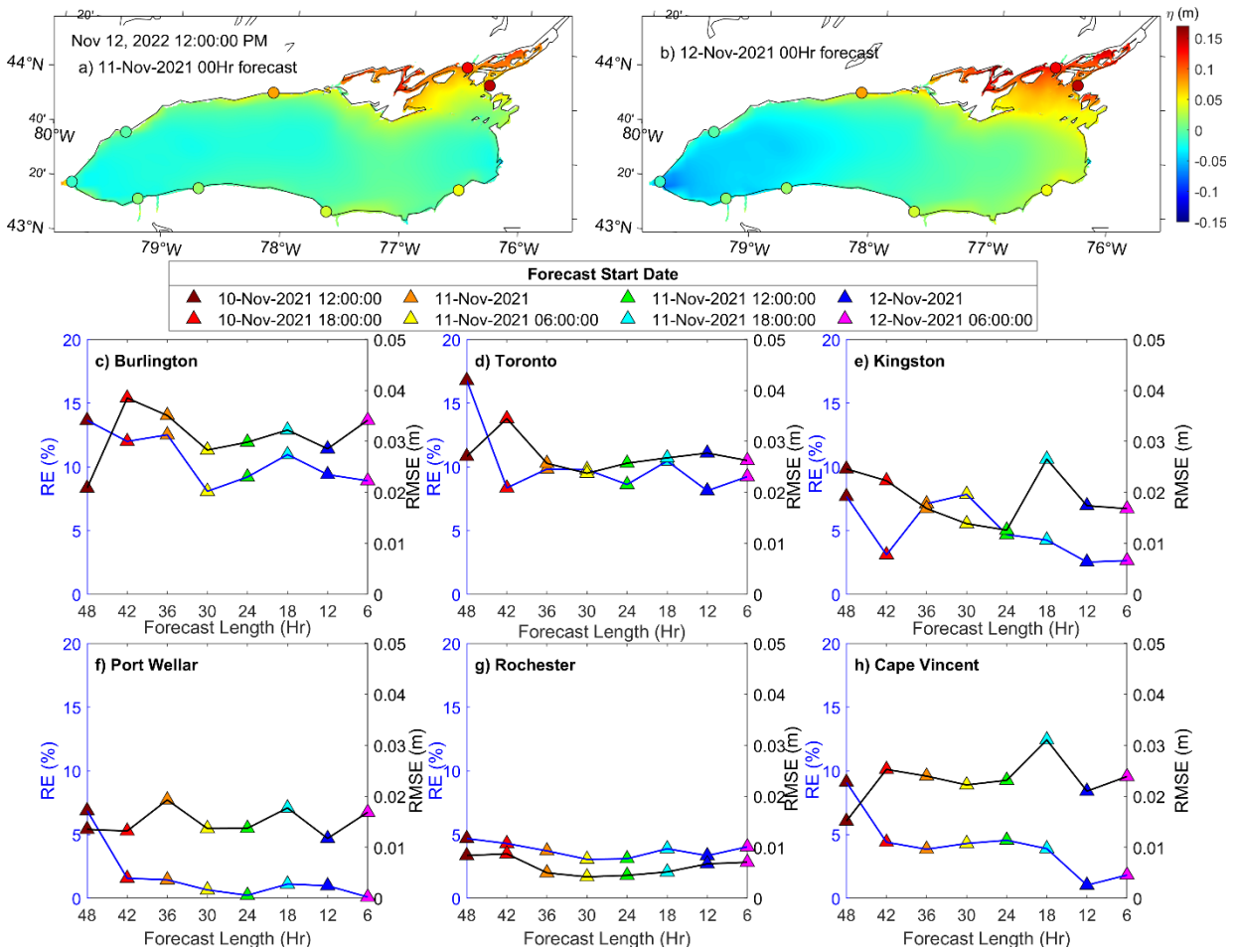
Figure 6: Contour plots showing maps of modelled water levels at the peak of the storm event from two different forecasts, with an a) 35 hr lead time starting November 11, 00:00 UTC and b) 11 hour lead time starting on November 12, 00:00 UTC, with observed data plotted at the observation locations in black circles. Panels c) to h) show metrics including the RE and RMSE for peak storm surge magnitude at the locations of 6 selected water level gauges from the 8 forecasts preceding the storm event.

Measured waves during this event reached up to 2.10 m, with the buoys in the western region of the lake (Fig. 7c, d) experiencing peak wave heights about 12 h earlier (Nov 11, 2021, 18:00 UTC) than the buoys in the eastern region of the lake (Fig. 7a, b; Nov 12 2021, 06:00 UTC). This is explained by the shift in wind direction over the storm duration, with winds originally from the southeast, rotating clockwise, then blowing dominantly from the west along the axis of the lake (Fig. S3 in the supplementary material). Overall, forecast simulations captured the magnitude of the waves all stations, with some error, and approximately 5 h delay in the timing of the peak H_s at Prince Edward Point (Fig. 7a). Error for waves during this event, at all stations, was constant for consecutive forecasts at all stations, with RMSE for

330   between 0.03 – 0.25 m and RE between 1-12%. Despite the generally consistent results, at the buoy

331   locations, maps from different forecasts show distinct changes between the 36 h forecast (Fig. 8a) and the

332   6 h forecast (Fig. 8b). Simulated wave fields in the northeast region of the lake showed similar results

333   between forecasts, but in the northwest, predicted wave magnitudes and directions were distinctly different.

334   The earlier forecast predicted waves under 0.70 m coming from the southeast, whereas the later forecast

335   showed larger waves ($H_s = 0.50 – 1.00$ m) from the southwest, which can be attributed to changes in

336   forecasted wind-fields.

337
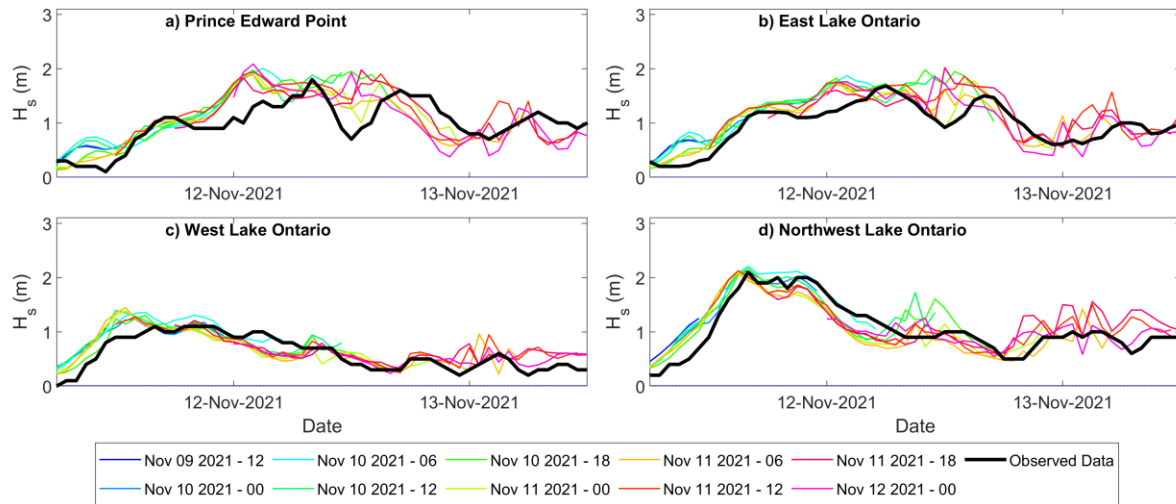
338

339   **Figure 7:** Time series of measured H_s at the location of the 4 buoys compared to modelled data from

340   progressive model forecasts for Event 1 (November 12, 2021).

341
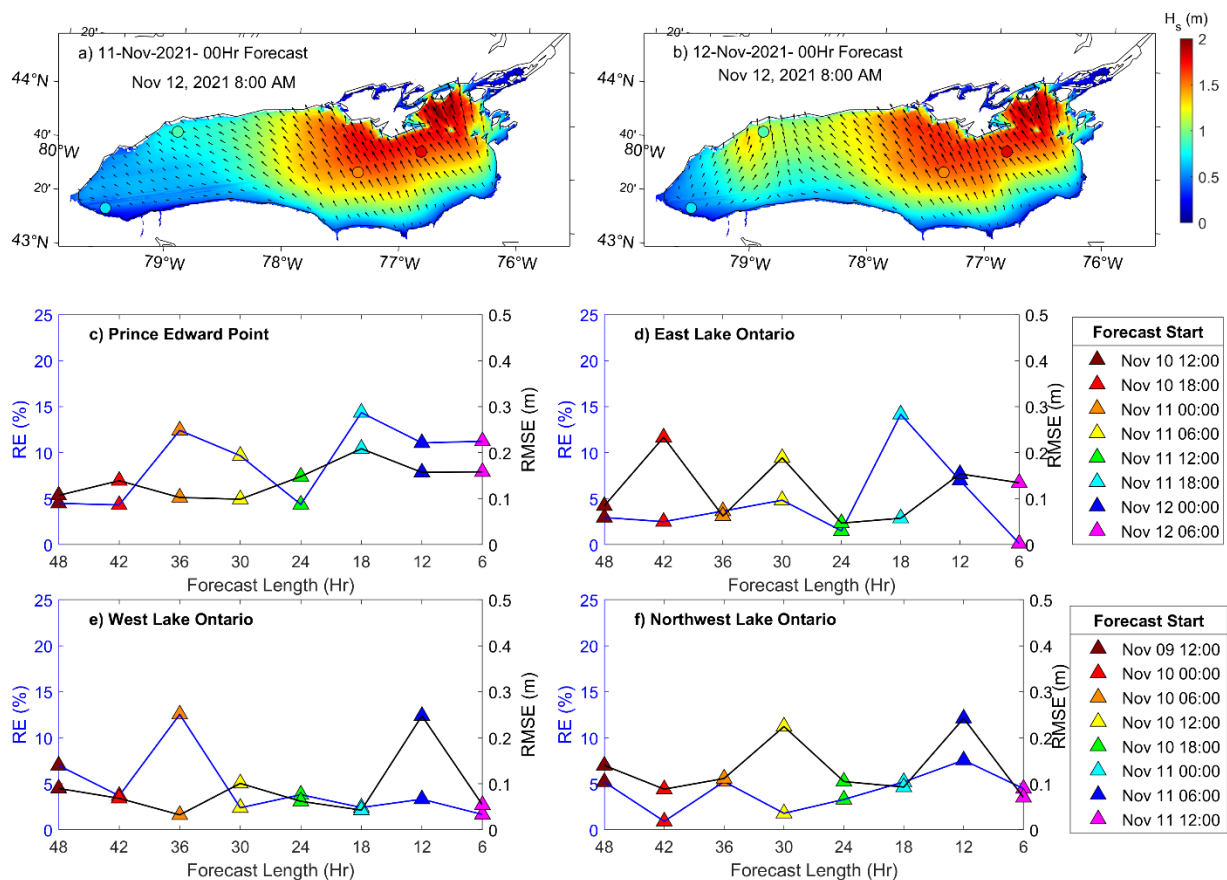
Figure 8: Contour maps of modelled waves with vectors indicating wave direction at a select time during the storm event from two forecasts, with: a) 32 hr lead time starting November 11, 00:00 UTC; and b) 8 hr lead time starting November 12, 00:00 UTC with observed data plotted at the observation locations in black circles. Every 10th vector is plotted for clarity. Panels c) to f) show metrics including the RE and RMSE for significant wave height at the locations of 4 buoys from the 8 forecasts preceding the storm event on November 12, 2021, 12:00 UTC, and RMSE values are computed over a 12 h period centered at the time of the peak H_s for each station.

For further investigation into model performance during storm events, wave forecasts during the event that resulted in the largest observed wave heights (December 1, 2022, Fig. 3c) were examined. During this storm, the lake experienced sustained easterly winds for almost 24 h, reaching speeds > 20 m s^{-1} on December 1, 14:00 UTC, generating waves > 4 m (Fig. 9. Data was only available from the one buoy at East Lake Ontario during this event, which recorded a maximum $H_s = 4.46$ m. The forecasts initially underestimated this value, with a maximum predicted wave height of $H_s = 4.19$ m from the forecast starting on November 29 18:00 UTC, and the next forecast then overestimated this value ($H_s = 4.54$ m). Subsequent

357 forecasts slightly underestimated the peak value, with the lowest predicted peak $H_s = 4.26$ m and the

358 maximum values occurring ~1 h after the observed peak. All forecast results tended to overestimate the

359 peak wave period, with predicted values ranging between 7.8 - 8.1 s, compared to an observed maximum

360 value of 7.2 s.

361
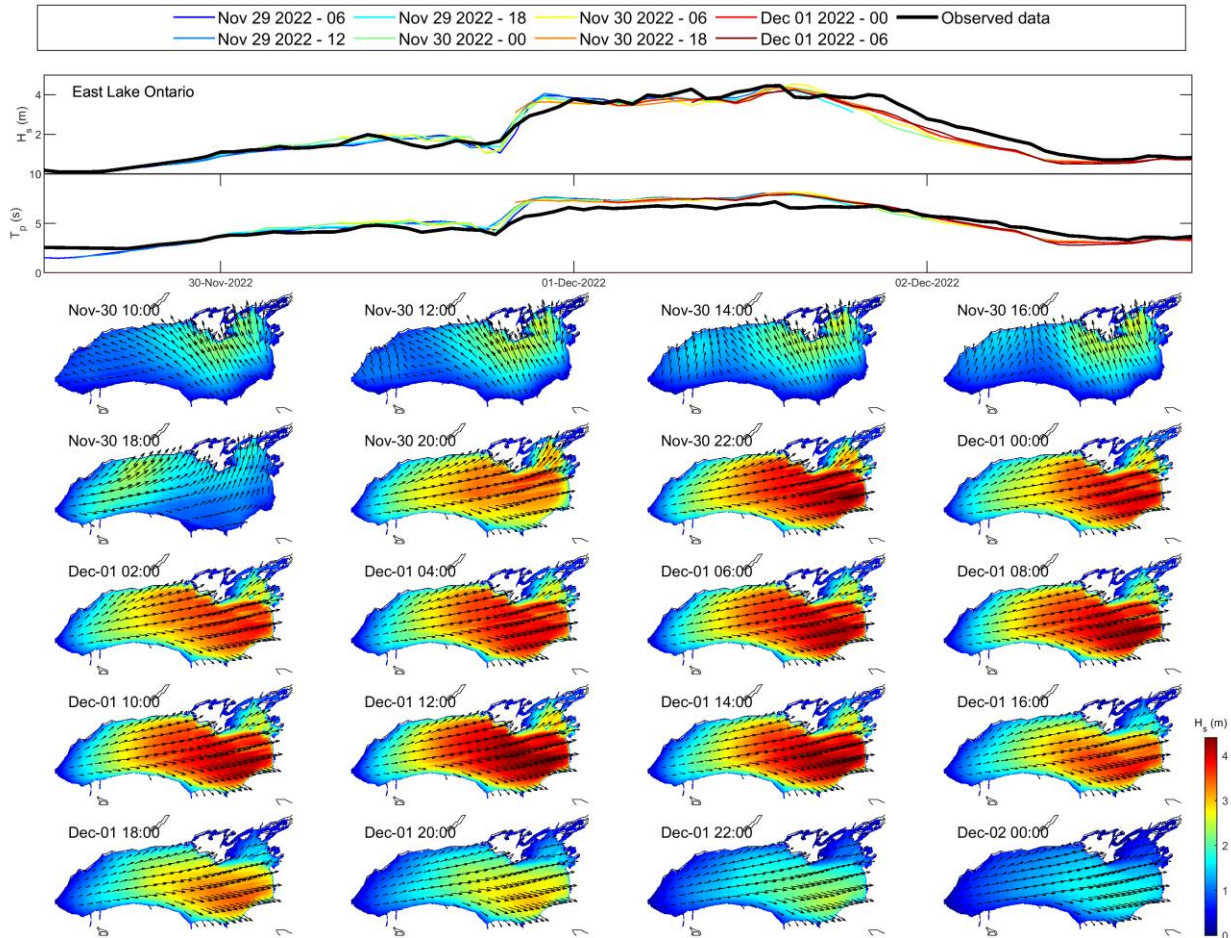
362

363 **Figure 9:** Variability in significant wave height during a storm event: measured H_s compared to progressive

364 forecast results at the Prince Edward Point Buoy for Event 3 (December 1, 2022; top) and maps of H_s and

365 wave direction shown at an interval of 2 h (every 10th vector is shown for clarity).

366

367 **4 Discussion**

368

369 *4.1. Forecast Lead Times*

Water level forecasts during a storm event on December 8, 2021, were examined in relation to forecast lead time. During this event, 21 m s^{-1} winds (Figure S4 in the supplementary material) generated a storm surge of approximately 0.20 m along the northeast coast, and a resulting setdown of 0.10 m on the opposite end of the lake. Error statistics throughout the peak of the event, as a function of forecast lead time, were plotted at selected stations (Fig. 10). The timing and magnitude of the storm surge was well represented by the forecast model, with RMSE < 0.05 m for all forecasts and a maximum RE =14%.
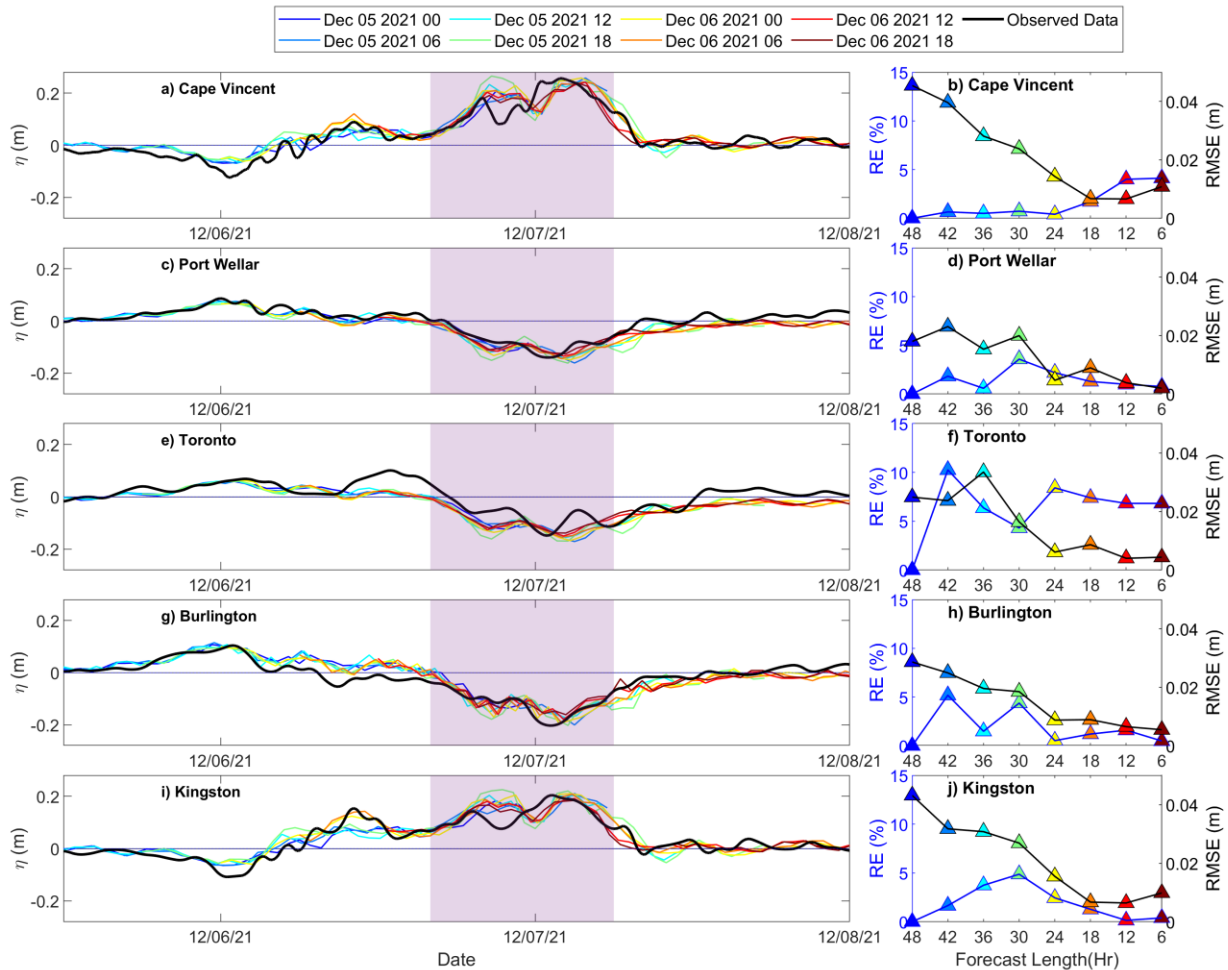
Figure 10: Time series of measured water levels at select observation points compared to forecasted data from progressive model simulations for Event 3: December 08, 2021, with corresponding plots showing computed RMSE calculated over the shaded area and percent error in peak storm surge from the 8 forecasts preceding the storm event.

Trends in the error can be identified for this event at all stations, with notable patterns corresponding to locations with larger fluctuations in water level (i.e., Cape Vincent, Kingston, Burlington). At these sites,

385 forecast error tended to decrease as the forecast length shortened. At Cape Vincent, the initial 48 h forecast
386 had an RMSE of 0.05 m and by the 18 h forecast, the RMSE had decreased to 0.01 m. However, after the
387 18 h forecast there was a slight increase in RE from less than 1% to about 5% (Fig. 10b). Trends in
388 decreasing error were also observed at Kingston, where a similar decrease in RMSE was observed, and the
389 RE was maintained between 1 – 5%, corresponding to a maximum underprediction of about 0.05 m (Fig.
390 10i, j). The locations with smaller ranges in surface fluctuations (Toronto, Port Wellar) generally showed
391 constant error (0.02 m and ~1% at Port Wellar; 0.01 m and 7% at Toronto) for consecutive forecast results
392 over the duration of this event (Fig. 10d, f).

393

394 Hydrodynamics in the model are only driven by atmospheric forcing, which is a primary source of
395 uncertainty in simulations of surface dynamics in large lakes. The accuracy of meteorological forecasts
396 typically decreases with increasing length due to assimilation schemes using observations and satellite
397 imagery to yield more accurate results (Buehner et al., 2015). Therefore, it is expected that hydrodynamic
398 forecast simulations will increase in accuracy as the lead time to a storm event decreases. For forecasts of
399 storm surges in other Great Lakes (e.g., Lake Erie; Lin et al., 2022) and coastal seas (e.g., Gulf of Mexico;
400 Dietrich et al., 2018), improvements in storm surge predictions are directly linked to increased accuracy in
401 meteorological forcing leading up to an event. However, our Lake Ontario model results do not follow a
402 consistent trend between different events, either improving (Fig. 10) or maintaining accuracy (Fig. 6;
403 Fig. 8). Cases where error increases (i.e. Fig 10b) or remains constant (i.e. Fig. 8), can be explained due to
404 sources of uncertainty in the model calibration and neglecting additional hydrodynamic processes in the
405 model setup (i.e. 3-dimensional circulation). Despite model accuracy being constant at the observation
406 locations, changes in the spatial variability of predicted water levels and wave conditions for different
407 forecasts are not clearly communicated through time series analysis but are qualitatively shown in maps of
408 results (Fig. 6; Fig. 10).

409

410 *4.2. Comparison with Other Models*

411 The current work (Coastlines-LO) makes use of a relatively simple, low computational demand modelling
412 approach. The performance of this model can be compared to the GLCFS, which delivers a higher resolution
413 and more complex forecast system in throughout the Great Lakes. Differences between predictions from
414 these models can be explained according to the setup of each system, including different hydrodynamic
415 models, grid resolutions, and atmospheric forcing inputs, which are summarized in table S3 in the
416 supplementary material. The GLCFS uses the 2 km horizontal resolution High Resolution Rapid Refresh
417 (HRRR) meteorological forcing, which is comparable to HRDPS (2.5 km), however previous studies have
418 found that wind and direction predictions can vary between these models (Rey and Mulligan, 2021;

419   Swatridge et al., 2022). The inclusion of waves in the two systems is also accounted for differently, with a
420   separate model (WaveWatch III) used to simulate waves in the GLCFS, while Coastlines-LO uses a
421   dynamically coupled wave and flow model that accounts for wave-current interactions. The inclusion of
422   wave coupling in simulations of the Great Lakes can impact water level predictions (Mao and Xia, 2017).
423   The GLCFS runs on NOAA's high performance computing system, and the larger computational power
424   allows it to include 3D baroclinic processes while still running in the required timeframe, whereas the
425   Coastlines-LO system in the present study uses a 2D, depth averaged approach, and therefore doesn't
426   resolve vertical gradients in lake temperature or 3D circulation. The inclusion of river inflows and outflows
427   in the GLCFS also allows the model to simulate seasonal changes in the mean lake water level instead of
428   accounting for these changes based on observed data in post-processing.

429

430   Forecasts results from both models were compared to observed data over a 6-day period in December 2022,
431   during which 2 storm events occurred (Fig. 11; Table S4 in the supplementary material). Results from the
432   first 6 h of subsequent forecasts are combined to construct a water level time series at observation points
433   for both models for the entire duration. Both models represent trends in water levels over this, resulting in
434   comparable metrics, with an average RMSE 0.02 m for both models, and r = 0.73 and 0.74 for Coastlines-
435   LO, and GLCFS, respectively. GLCFS achieved better predictions of peak water levels at Oswego for the
436   event on December 1(RE = 30% for GLCFS, RE = 51% for Coastlines-LO; Fig. 11a), and more accurately
437   represented the surface fluctuations observed over the entire 6 day period at Toronto (Fig. 11f).While
438   GLCFS was able to represent water levels at some locations, Coastlines-LO had higher accuracy predictions
439   at others (Fig. 11c, d). At Port Wellar and Cape Vincent, Coastlines-LO better predicted the peak set-down
440   and set-up on December 1 by 0.01 m and 0.03 m respectively, while GLCFS underpredicted at these
441   locations by 0.05 m and 0.09 m. Boths models had difficulty simulating the second storm surge (December
442   3) at Oswego and Cape Vincent (Fig. 11 a, c), where the observed surge occurs approximately 3 h before
443   the predicted peak. At the Kingston station (Fig. 11h), storm surges of 0.25 m and 0.30 m are observed.
444   Coastlines-LO yielded better predictions for the first event, simulating a peak value of 0.24 m, compared
445   to 0.28 m predicted by GLCFS, while GLCFS performed better for the second event, with a predicted storm
446   surges of 0.28 m and 0.22 m for GLCFS and Coastlines-LO, respectively. Therefore, while the GLCFS
447   offers several advantages, Coastlines-LO provides comparable results for water level prediction with a
448   lower computational demand. This demonstrates that a relatively simple modelling system can be applied
449   to coastal environments to achieve accurate and efficient hydrodynamic predictions. The open-source and
450   flexible wrapper code could therefore be theoretically adapted to include different hydrodynamic models
451   and investigate different field sites as previous works have successfully applied similar approaches for
452   forecast modelling (e.g., Lin et al., 2022; Rey and Mulligan 2021).

453
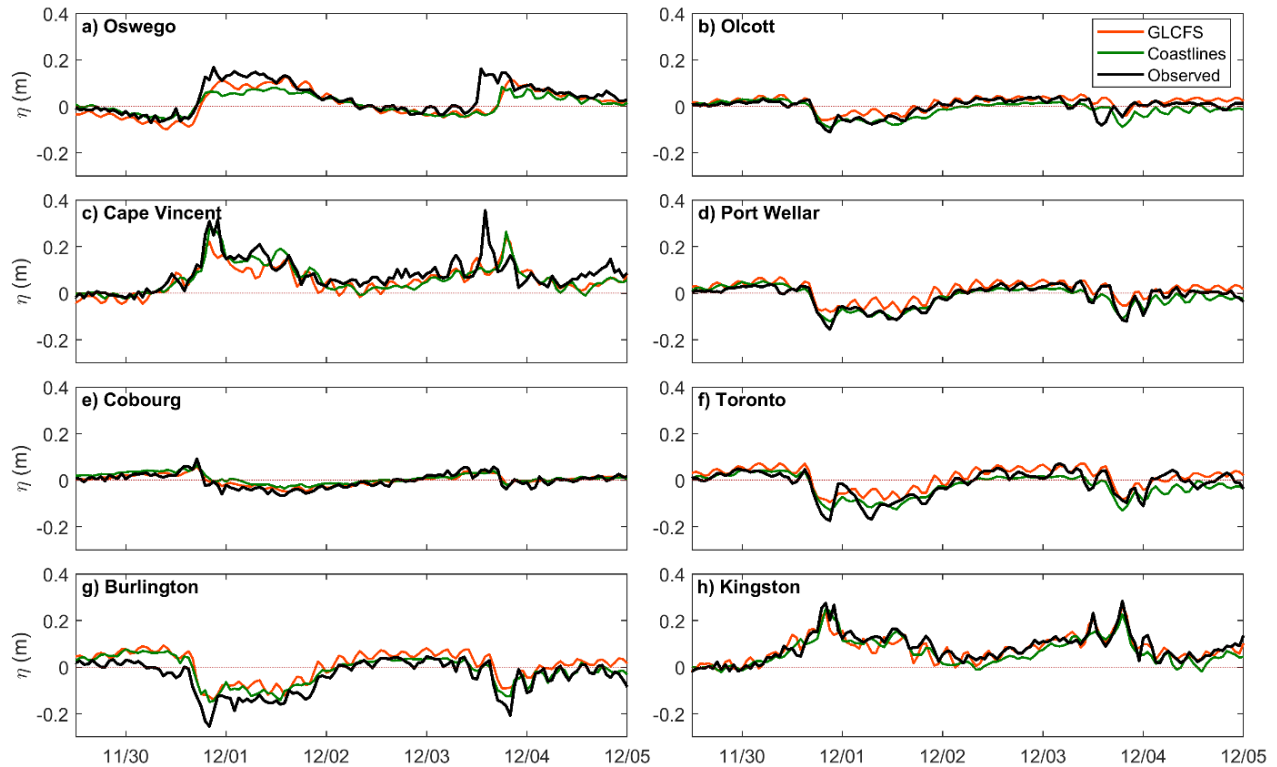
Figure 11: Compiled Coastlines-LO forecast results compared to forecasts from the GLCFS and observed data at select water level gauge locations interpolated to a 30 minute time resolution for 2 subsequent events between November 30 – December 5, 2022.

4.3. Limitations and Uncertainties

Sensitivity testing and calibration of the numerical model this system is based on, comes from the work of Swatridge et al. (2022), which found that 3D simulations of Lake Ontario improved predictions of surface behaviour compared to 2D depth averaged simulations. The 3D simulation allowed the model to account for transfer of surface momentum into baroclinic motions, giving a better representation of current velocities and surface seiching following a storm event, resulting in reduced RMSE during storm events by up to 12%, and improvement in modelled peak storm surge magnitude by up to 0.03 m. While 3D simulations improved accuracy, they also increased the computational runtime of a 24 h simulation from about 2.5 h to 4 h. Ten-day forecasts of 3D hydrodynamic processes in Lake Erie has been achieved by Lin et al. (2022) in using the AEM3D model with a similar Coastlines computational workflow as the current work; however, the Lake Erie model in on a coarser 2 km horizontal grid and does not couple with SWAN to predict surface waves, which is computationally expensive compared to hydrodynamic simulations. Therefore, to apply this model in real-time with a new simulation every 6 h, 2D simulations are used, potentially resulting in up to 12% greater uncertainty in the forecast results. Additional investigation of

471 real-time model performance during more storm events, including when the lake is stratified is
472 recommended for further model validation.

473

474 There is additional uncertainty in model results during the winter season, when ice forms in the Great Lakes.
475 Lake Ontario typically experiences some ice cover between December and April (Anderson et al., 2018),
476 which impacts lake processes, including water levels, circulation, and waves through limited air-water
477 momentum transfer (Anderson et al., 2018; Farhadzadeh and Gangai, 2017). While ice cover has been
478 simulated in Lake Ontario using other models (e.g., Oveisy et al., 2012), it is presently not available in
479 Delft3D-SWAN. Therefore, simulations of surface behaviour during the ice-covered months would have
480 limited accuracy in ice-covered areas. Future work could incorporate ice cover into the model by applying
481 dynamic masking of ice-covered surfaces using satellite data to improve results during these months.

482

483 While this system requires low computational resources, making it flexible for adaption to other coastal
484 regions, its capability for forecasting in additional locations is an area that requires future investigation.
485 The applicability of the model is limited by the availability of online data for model forcing and validation.
486 In order to account for seasonal changes in mean lake levels, near real-time measurements of water levels
487 are needed in the simulation to adjust the datum in post-processing. However, if no data were available the
488 simulation could include the wind-generated short-term fluctuations in surface levels and real-time
489 operations could continue. The workflow of the model is also limited by the availability of atmospheric
490 forcing data, with any interruptions of service in the HRDPS forecasts causing the hydrodynamic
491 simulations to fail for that run-cycle. Improvements in the system could account for this by providing a
492 secondary source of atmospheric forcing in that case. In future studies, we recommend applying this system
493 to a region in the coastal ocean, therefore requiring the development of real-time forecast inputs of open
494 boundary conditions.

495

496 **5 Conclusions**

497

498 A forecast model for wind-driven hydrodynamics was developed and applied to Lake Ontario using an
499 approach with relatively low computational demand. Wind-waves and water levels were simulated using a
500 dynamically coupled Delft3D-SWAN model driven by high resolution atmospheric forcing. Simulations
501 were able to forecast the wind-driven variability in the lake surface, with seasonal changes in the total water
502 levels accounted for by adjusting the datum for each forecast cycle based on observations of the mean water
503 level. The system provides rapid (~5 h runtime) predictions that are publicly available through the project
504 webpage, with the automated system forecasting a 48 h period every 6 h. The model has been running

continuously since April 2021, capturing a variety of storm events with storm surges up to 0.30 m and significant wave heights over 4.00 m. Reliable prediction for wave conditions during winter months are provided by the forecast model when no wave observations are available, however accuracy is limited where ice is present as this process is not included in the modelling system.

Results show that the model is effective in simulating short term fluctuations in the water levels and wave conditions during strong storm events, with relative errors between observed and forecasted storm surge magnitudes and significant wave heights of less than 15%. Larger errors typically corresponded to locations in the lake with larger ranges in observed water levels. For storm events, as the forecast lead time decreases for progressing forecasts, the simulated results changed as a result of updates to the meteorological forcing. No constant trends in forecast error due to decreasing forecast length were apparent, with forecast accuracy increasing with shorter forecasts in some cases and staying constant at others, but overall results agreed well with observed data for all forecasts leading up to an event, with RMSE for storm surge and waves below 0.05 m and 0.30 m, respectively. The model compared well with other existing forecast models in the Great Lakes (GLCFS), yielding comparable results for water level predictions during multiple storm events. Due to the low computational requirements and pan-Canadian coverage from the High Resolution Deterministic Prediction System forecasts, this model could be adapted to other Canadian lakes and coastal seas with available bathymetry data for storm surge prediction and monitoring.

6 Code and Data Availability Statement

Real-time model results are available at https://coastlines.engineering.queensu.ca/lake-ontario/, and archived on the local server, to be made available by contacting the corresponding author. HRDPS input data is available from the Meteorological Service of Canada Datamart and observed data is openly accessible online, as cited in the text. The source code and documentation of the open source numerical model (Delft3D 4.01.01) can be accessed on their online repositories (https://oss.deltares.nl/web/delft3d/source-code, last access: 19 December, 2023). The Python and MATLAB scripts, and supporting files used in the automated workflow, as well as data and scripts used to generate the plots presented in this paper are archived on Zenodo (https://doi.org/10.5281/zenodo.10407863, Swatridge, 2023).

7 Author contributions

The concept of the COASTLINES-LO workflow was designed by RM, LB, SS, and LS, and LS implemented the idea. LS developed the performed the model simulations. All authors contributed to the validation of the model and interpretation of the results. LS wrote the manuscript with contributions from LB, SS, and RM.

8. Competing Interests

The contact author has declared that neither they nor their co-authors have any competing interests.

9 Acknowledgments

Funding for this research was provided by Natural Sciences and Engineering Research Council of Canada (NSERC) under the Discovery Grant program awarded to R.P. Mulligan (RGPIN/04043-2018), and a Queen's Dean's Research Fund award to L. Boegman, R.P. Mulligan and S. Shan.

10. References

Anderson, E. J., Fujisaki-Manome, A., Kessler, J., Land, G.A., Chu, P.Y., Kelley, J.G.W., Chen, Y., and Wang, J.: Ice Forecasting in the Next-Generation Great Lakes Operational Forecast System (GLOFS). J. Mar. Sci. Eng., 6(4), 123, https://doi.org/10.3390/jmse6040123, 2018.

Asher, T.G., Luettich, R.A., Fleming, J.G., and Blandton, B.O.: Low frequency water level correction in storm surge models using data assimilation. Ocean Modelling, 144, https://doi.org/10.1016/j.ocemod.2019.101483, 2019.

Baracchini, T., Wuest, A., and Bouffard, D.: Meteolakes: An operational online three-dimensional forecasting platform for lake hydrodynamics. Water Research, 172.1-12, https://doi.org/10.1016/j.watres.2020.115529, 2020.

Bender, M.A., Knutson, T.R., Tuleya, R.E., Sirutis, J.J., Vecchi, G.A., Garner, S.T. and Held, I.M.: Modeled impact of anthropogenic warming on the frequency of intense Atlantic hurricanes. Science, 327(5964), 454-458, DOI: 10.1126/science.1180568, 2010.

Bilskie, M.V., Asher, T.G., Miller, P.W., Fleming, J.G., Hagen, S.C. and Luettich Jr. , R.A.: Real-time simulated storm surge predictions during Hurricane Michael (2018), Wea. Forecasting, 37, 1085–1102, https://doi.org/10.1175/WAF-D-21-0132.1, 2022.

Buehner, M., McTaggart-Cowan, R., Beaulne, A., Charette, C., Garand, L., Heilliette, S., et al.: Implementation of Deterministic Weather Forecasting Systems Based on Ensemble-Variational

Data-Assimilation at Environment Canada. Part 1: The Global System, Mon. Wea. Rev., 143, 2532–2559, https://doi.org/10.1175/MWR-D-14-00354.1, 2015.

Booij, N., Ris, R.C., and Holthuijsen, L.H.: A third-generation wave model for coastal regions: 1.Model Description and validation. Journal of Geophysical Research: Oceans, 104(C4), 7649-7666, https://doi.org/10.1029/98JC02622, 1999.

Carey, C.C., Woelmer, W.M., Lofton, M.E., Figueiredo, R.J., Bookout, B.J., Corrigan, R.S., et al.: Advancing lake and reservoir water quality management with near-term iterative ecological forecasting, Inland Waters, 12(1), 107-120, https://doi.org/10.1080/20442041.2020.1816421, 2022.

Chisholm, L., Talbot, T., Appleby, W., Tam, B., and Rong, R.: Projected change to air temperature, sea-level rise, and storms for the Gulf of Main region in 2050, Elem Sci Anth. 9(1), 1-14, https://doi.org/10.1525/elementa.2021.00059, 2021.

Cooper, A.H., and Mulligan, R.P.: Application of a Spectral Wave Model to assess Breakwater Configurations at a small craft harbour on Lake Ontario, J. Mar. Sci. Eng., 2016, 4(3), 46, https://doi.org/10.3390/jmse4030046, 2016,

Danard, M., Munro, A., and Murty, T.: Storm surge hazard in Canada. Natural Hazards, 28, 407–434, https://doi.org/10.1023/A:1022990310410, 2003.

Dietrich, J. C., Muhammad, M., Curcic, M., Fathi, A., Dawson, C. N., Chen, S. S., and Luettich Jr., A.: Sensitivity of Storm Surge Prediction to Atmospheric Forcing during Hurricane Isaac, J. Waterway, Port, Coastal, and Ocean Eng, 144(1), https://doi.org/10.1061/(ASCE)WW.1943-5460.0000419, 2018.

Elko, N., Dietrich, C., Cialone, M.A., Stockdon, H., Bilksie, M. W., Boyd, B., Charbonneau, B., Cox., D., Desback, K., Elgar, S., Lewis, A., Limber, P., Long, J., Massey, C., Mayo, T., McIntosh, K., Nadal-Caraballo, N.C., Raubenheimer, B., Tomiczek, T., Wargula, A. E. (2019). Advancing the understanding of storm processes and impacts. Shore & Beach, 87(1).

Farhadzadeh, A., and Gangai, J.: Numerical Modelling of Coastal Storms for Ice-Free and Ice-Covered Lake Erie, J. of Coastal Research, 33(6), 1383-1396, https://doi.org/10.2112/JCOASTRES-D-16-00101.1, 2017.

FEMA: FEMA Great Lakes Coastal Guidelines, Appendix D.3 Update. FEMA, 2014.

Forbes, C., Luettich, R.A., Mattocks, C.A., and Westerink, J.J.: A retrospective evaluation of the storm surge produced by Hurricane Gustav (2008): Forecast and hindcast results, Wea. Forecasting, 25(6), 1577–1602, https://doi.org/10.1175/2010WAF2222416.1, 2010.

603 Fleming, J.G., Fulcher, C.W., Luettich Jr., R.A., Estade, B.D., Allen, G., and Winer, H.S.: A real time storm
604   surge forecasting system using ADCIRC, Proceedings of the International Conference on Estuarine
605   and Coastal Modeling, https://doi.org/10.1061/40990(324)48, 2008.

606 Gallagher, G.W., Duncombe, R.K., and Steeves, T. M.: Establishing Climate Change Resilience in the
607   Great Lakes in Response to Flooding, Journal of Science Policy & Governance, 17(1),
608   https://doi.org/10.38126/JSPG170105, 2020.

609 Gronewold, A.D., and Rood, R.B.: Recent water level changes across Earth's largest lake system and
610   implications for future variability, J. of Great Lakes Research, 45(1), 1-3,
611   https://doi.org/10.1016/j.jglr.2018.10.012, 2019.

612 Gronewold, A.D., Fortin, V., Lofgren, B., Clites, A., Stow, C.A., and Quinn, F.: Coasts, water levels, and
613   climate change: A Great Lakes perspective, Climate Change, 120, 697-711,
614   https://doi.org/10.1007/s10584-013-0840-2, 2013.

615 Huang, A., Rao, Y.R., Lu, Y., and Zhao, J.: Hydrodynamic modelling of Lake Ontario: An intercomparison
616   of three models. Journal of Geophysical Research: Oceans, 115(C12), 1-16,
617   https://doi.org/10.1029/2010JC006269, 2010.

618 Kelley, J.G.W., Chen, Y., Anderson, E.J., Lang, G.A., and Xu, J.: Upgrade of NOS Lake Erie Operational
619   Forecast System (LEOFS) to FVCOM: Model Development and Hindcast Skill Assessment; NOS
620   CS 40, NOAA; NOAA Technical Memorandum, http://doi.org/10.7289/V5/TM-NOS-CS-40,
621   2018.

622 Lacke, M. C., Knox, J. A., Frye, J. D., Stewart, A. E., Durkee, J. D., Fuhrmann, C. M., & Dillingham, S.
623   M. (2007). A climatology of cold-season non convective wind events in the Great Lakes region.
624   Journal of Climate, 20(24), 6012-6022. https://doi.org/10.1175/2007JCLI1750.1

625 Lesser, G.R., Roelvink, J.A., and Stelling, G.S.: Development and validation of a three-dimensional
626   morphological model, Coastal Engineering, 51(8-9), 883-915,
627   https://doi.org/10.1016/j.coastaleng.2004.07.014, 2004.

628 Lin, S., Boegman, L., Shan, S., and Mulligan, R.P.: An automatic lake-model application using near real-
629   time data forcing: Development of an operational forecast workflow (COASTLINES) for Lake
630   Erie, Geosci. Model Dev, 15(3), 1331-1353, https://doi.org/10.5194/gmd-15-1331-2022, 2022.

631 McCombs, M.P., Mulligan, R.P., Boegman, L., and Rao, Y.R.: Modelling surface waves and wind-driven
632   circulation in eastern Lake Ontario during winter storms, J. Great Lakes Res., 40(3), 130-142,
633   https://doi.org/10.1016/j.jglr.2014.02.009, 2014a.

634 McCombs, M.P., Mulligan, R.P., and Boegman, L.: Offshore wind farm impacts on surface waves and
635   circulation in Eastern Lake Ontario, Coastal Engineering, 93, 32-39,
636   https://doi.org/10.1016/j.coastaleng.2014.08.001, 2014b.

Mao, M., and Xia, M.: Dynamics of wave-current-surge interactions in Lake Michigan: A model comparison, Ocean Modelling, 110, 1-20, https://doi.org/10.1016/j.ocemod.2016.12.007, 2007.

Milbrandt, J.A., Belair, S., Faucher, M., Vallee, M., Carrera, M.L., and Glazer, A.: The Pan-Canadian High Resolution (2.5 km) Deterministic Prediction System, Weather and Forecasting, 31(6), 1791-1816, https://doi.org/10.1175/WAF-D-16-0035.1, 2016.

Oveisy, A., Boegman, L., and Imberger, J.: Three-dimensional simulation of lake and ice dynamics during winter, Limnol Oceanogr, 57(1), 43-57, https://doi:10.4319/lo.2012.57.1.0043, 2012.

Paramygin, V.A., Sheng, Y.P., and Davis, J.R.: Towards the development of an operational forecast system for the Florida coast, J. Mar. Sci. Eng., 5(1), https://doi.org/10.3390/jmse5010008, 2017.

Paturi, S., Boegman, L., and Rao, Y.R.: Hydrodynamics of eastern Lake Ontario and the upper St. Lawrence River, J. Great Lakes Res., 38(4), 194-204, https://doi.org/10.1016/j.jglr.2011.09.008, 2012.

Peng, M., Zhang, A., Anderson, E.J., Lang, G.A., Kelley, J.G.W., and Chen, Y.: Implementation of the Lakes Michigan and Huron Operational Forecast System (LMHOFS) and the Nowcast/Forecast Skill Assessment, NOAA technical report NOS CO-OPS, 2019.

Prakash, S., Atkinson, J.F., and Green, M.L.: A semi-Lagrangian study of circulation in Lake Ontario, J. Great Lakes Res., 33(4), 774-790, https://doi.org/10.3394/0380-1330(2007)33[774:ASSOCA]2.0.CO;2, 2007.

Rey, A.J.M., and Mulligan, R.P.: Influence of hurricane wind field variability on real-time forecast simulations of the coastal environment, Journal of Geophysical Research: Oceans, 126(1), 1-20, https://doi.org/10.1029/2020JC016489, 2021.

Shore, J.A.: Modelling the circulation and exchange of the Kingston Basin and Lake Ontario with FVCOM, Ocean Modelling, 30(2-3), 106-114, https://doi.org/10.1016/j.ocemod.2009.06.007, 2009.

Sogut, D.V., Jensen, R.E., and Farhadzadeh, A.: Characterizing Lake Ontario Marine Renewable Energy Resources, Marine Technology Society Journal, 53(2), 21-38, https://doi.org/10.4031/MTSJ.53.2.3, 2019.

Steinschneider, S.: A hierarchical Bayesian model of storm surge and total water levels across the Great Lakes shoreline – Lake Ontario, J. Great Lakes Res. 47(3), 829-843, https://doi.org/10.1016/j.jglr.2021.03.007, 2021.

Studholme, J., Fedorov, A.V., Gulev, S.K., Emanuel, K., and Hodges, K.: Poleward expansion of tropical cyclone latitudes in warming climates, Nature geoscience, 15, 14-18, https://doi.org/10.1038/s41561-021-00859-1, 2022.

Swatridge, L.L., Mulligan, R.P., Boegman, L., Shan, S., and Valipour, R.: Coupled modelling of storm surge, circulation, and surface waves in a large, stratified lake, J. Great Lakes Res, 48(6), 1520-1535, https://doi.org/10.1016/j.jglr.2022.08.023, 2022.